

Current-voltage curves for molecular junctions: the effect of substituents

Charles W. Bauschlicher, Jr.* and John W. Lawson†

Mail Stop 230-3

Center for Advanced Materials and Devices

NASA Ames Research Center

Moffett Field, CA 94035

Abstract

We present current-voltage (I-V) curves for phenylene ethynylene oligomers between two Au surfaces computed using a Density Functional Theory/Greens Function approach. In addition to the parent molecule, two different substituents are considered: one where all the hydrogens are replaced by chlorines and a second where one H is replaced by an NO₂ group. In this way, we can study the difference between electron withdrawing and π orbital effects. For low biases, a reduced current for the derived species is consistent with a shift of HOMO to lower energy due to the electron withdrawal by Cl or NO₂. At higher biases, the LUMO becomes important, and the Cl and NO₂ substituted species carry more current than the parent because the LUMO is stabilized (shifted to lower energy) due to the withdrawal of electrons by the Cl and NO₂. In these molecules, the C₂ bridging units as well as the thiol anchor group are shown to create bottlenecks to current flow.

I. INTRODUCTION

Molecular electronics is a relatively new area, but already many interesting effects have been observed. One of the more interesting discoveries has been the negative differential resistance (NDR) found for a phenylene ethynylene trimer, with an NO_2 side group, on a gold surface¹, see molecule III in Fig. 1, which we denote as $\text{M}(\text{NO}_2)$. In contrast, the parent molecule with all hydrogen atoms (molecule I, which we denote as $\text{M}(\text{H})$) does not show NDR. Since the $\text{M}(\text{NO}_2)$ derivative can have high or low current flow states, it can be used to store a bit, as Reed and co-workers² have demonstrated; they read and wrote a bit using such a molecular device.

There have been two interesting theoretical investigations^{3,4} of related molecules. Taylor et al.³ studied molecules $\text{M}(\text{H})$ and $\text{M}(\text{NO}_2)$ between two Au surfaces and found very similar current-voltage (I-V) curves for these two molecules. More recently Yin et al.⁴ studied molecule $\text{M}(\text{H})$ and species related to $\text{M}(\text{NO}_2)$. They found that adding NO_2 to the central benzene ring and an NH_2 group to either the central or end benzene rings increased the current flow relative to the unsubstituted species. They concluded that the conduction was through the lowest unoccupied orbital (LUMO) and the NO_2 shifts the LUMO to lower energy and hence the current increases relative to $\text{M}(\text{H})$. Since NH_2 has little effect on the LUMO, their results suggest that $\text{M}(\text{NO}_2)$ would carry more current than $\text{M}(\text{H})$. Yin et al. also noted that the addition of NO_2 significantly affected the shape of the highest occupied molecular orbital (HOMO), but that it is difficult to directly relate the nature of the orbitals to the I-V curves. We made the same observation for related molecular systems⁵. In this manuscript we compare the I-V curves for the three related molecules shown in Fig. 1. Molecule II, which we denote as $\text{M}(\text{Cl})$, has not been studied experimentally, but it is studied here because it is expected to shift the orbital energies relative to $\text{M}(\text{H})$, like molecule $\text{M}(\text{NO}_2)$. However, $\text{M}(\text{Cl})$ is not expected to affect the character of the π orbitals as found for $\text{M}(\text{NO}_2)$. That is, a comparison of $\text{M}(\text{Cl})$ and $\text{M}(\text{NO}_2)$ can yield some insight into electron withdrawing and π orbital effects.

II. METHODS

The I-V curves are computed using the self-consistent, non-equilibrium, Green's function approach as implemented by Xue, Datta, and Ratner^{6,7,8,9,10}. Our approach has been described in detail in previous work and we only summarize it here. We include six Au atoms from each surface in our treatment of the extended molecule. The extended molecule is coupled to two semi-infinite gold (111) surface with the 6 Au atoms removed, whose effects are included as self-energy operators through a recursive Green's function procedure. The coupling between the bulk contacts and the extended molecule is determined using a tight-binding approach^{7,11}, where an additional 27 gold atoms in each contact are coupled directly to the extended molecule. Thus the calculations correspond to a single isolated bridging molecule between two Au(111) surfaces and not to a calculation including periodic boundary conditions.

The extended-molecule electronic structure calculations are based on density functional theory (DFT), using the pure BPW91^{12,13} functional. The α and β spin densities are constrained to be equal in the extended molecule calculations. The Au atoms are described using the Los Alamos effective core potential¹⁴ with 11 valence electrons. As in previous work, the most diffuse s, p, and d primitives are deleted from the associated valence basis set, and the remaining primitives are contracted to a minimal basis set. The C, O, N, Cl, and S atoms are described using the compact effective core potential and the associated 121G basis set¹⁵, i.e. the CEP-121G basis set. A d polarization function is added¹⁶ to the C, O, N, Cl, and S atoms, and diffuse functions are added to O, N, Cl and S. The hydrogen set is the 6-311G set developed by Pople and co-workers¹⁶. This valence triple zeta basis set is the VTZ+P set used in most of our previous work. We use a temperature of 300 K in the Green's function calculations.

We should note that in previous work^{17,18} we considered larger metal clusters and, while I-V curves obtained using the Au₆ clusters are not completely converged with respect to the size of the metal cluster, they are qualitatively correct. Because the three molecules considered in this work are similar and we are interested in relative

differences, the use of the Au₆ clusters is a good compromise between accuracy and computational expense.

The bridging species studied are derived from the three molecules shown in Fig. 1. Their geometry is optimized at the B3LYP/6-31G* level^{16,19,20}. The terminal H atoms were removed and the fragment is connected to the two Au(111) surfaces. The C₂ axis of the molecular fragment is perpendicular to the surfaces and the S atoms are placed above a three-fold hollow at a distance of 1.905 Å above the Au surface. We should note that a full optimization of M(NO₂) results in a back bone that is not linear, so the optimization is constrained so that the C₂ axes of the benzene rings and the connecting C₂ units are all colinear. This is consistent with the other studies.

We report results for both zero bias transmission functions as well as full I-V characteristics. The transmission function is calculated using the Landauer equation $T(E) = Tr[\Gamma_R G \Gamma_L G^\dagger]$ where Γ_R, Γ_L are the coupling functions for the right and left contacts. The current is evaluated as an integral of $T(E)$ in an energy window around the Fermi level,

$$I = \frac{2e}{h} \int_{-\infty}^{\infty} T(E) \times [f(E - \mu_l) - f(E - \mu_r)] dE,$$

where f is the Fermi function. The current is of direct interest since it corresponds to an experimentally observable quantity. The transmission spectrum, while directly related to the current, also contains important microscopic information.

In this work we compute the change in some properties, like the charge density and electrostatic potential, due to contact formation. These are computed as the property of the extended molecule (connected to the bulk at zero bias) minus the property of the free molecule minus the property of the two Au₆ clusters (connected to the bulk).

The electronic structure calculations are performed using the Gaussian03 program system²¹. All of the Green's function calculations are performed using the code described previously^{6,7,8,9,10} that has been modified for the hybrid and analytic integration¹⁸.

III. RESULTS AND DISCUSSION

The electron affinities (EAs) and selected orbital energies of the three molecules studied in this work are given in Table 1. We first note that the EA values are $M(\text{H}) < M(\text{NO}_2) < M(\text{Cl})$, and the orbital energies are consistent with the EA values. Namely, the twelve Cl atoms withdraw more electrons from the rings than the one NO_2 group, which withdraws more than the all hydrogen atom case. This electron withdrawal stabilizes the orbitals of $M(\text{Cl})$ the most, followed by $M(\text{NO}_2)$ and lastly by $M(\text{H})$.

We plotted the orbitals of the free molecules and the extended molecule (i.e. the bridging molecule connected to two Au_6 clusters). Since neither set of orbitals appears to offer great insight into the conduction, we do not show the plots, but we note the character of the orbitals. First considering the free molecule orbitals. The HOMO and LUMO for molecules $M(\text{H})$ and $M(\text{Cl})$ shows that they are delocalized and are very similar in character, with the LUMOs being even more similar than the HOMOs. That is, substituting Cl for H has shifted the orbital energies, but has not significantly affected the nature of the HOMO and LUMO. For molecule $M(\text{NO}_2)$, Yin et al.⁴, who found that the HOMO was localized mostly on the NO_2 group and the LUMO was delocalized, while at the level of theory used in our work, our HOMO is delocalized, but our LUMO is localized. Clearly, the localization depends on the choice of functional used. Using the extended molecule orbitals, one finds that the HOMO and HOMO-1 of all three molecules are essentially metal-S sigma bonds. The HOMO-2 is a π orbital on the bridging molecule, with a sizable component on the metal, and looks very similar for all three molecules. The LUMO is a π orbital and also looks very similar for all three molecules considered. A notable difference for the three molecules is the LUMO+1 for $M(\text{NO}_2)$ which is mostly localized on the NO_2 group.

When the molecules are connected to the bulk and an electric field is applied, the orbitals will mix, making it difficult to interpret how the nature of the molecular orbitals will affect the I-V curves. To obtain a more accurate picture of the factors affecting conduction, we investigate properties computed with the molecule connected

to the bulk. We computed both the change in charge density and in the electrostatic potential energy due to contact formation. Since the information obtained from both properties is similar, we plot only the electrostatic potential energy in Fig. 2. The electrostatic potential energy for molecule M(H) with the z-coordinate integrated out is shown in Fig. 2a, while in Fig. 2b we compare the change in electrostatic potential energy for all three molecules along the axis of the molecule. For M(H) there are large changes at the ends of the molecule, but there are also sizable changes at the C₂ bridging units; not surprisingly, there were changes in the charge density at the same two locations. It is not too surprising to see large changes were the Au-S bond forms and even some changes on the benzene ring nearest the S atoms. However, we find it somewhat unexpected that the C₂ bridging units show larger changes than some of the C atoms in the end benzene rings. It appears that forming the Au-S bond has affected the electrostatic potential (and charge density) throughout the molecule. Fig. 2b shows that M(H) and M(NO₂) are fairly similar, however, it is perhaps a bit surprising that the biggest differences are at the ends of the molecule and not in the center where the NO₂ is located. The plot for M(Cl) shows larger differences with M(H) than does M(NO₂), which is consistent with larger electron withdrawing power of the Cl leading to larger changes for the M(Cl) density compared with M(H) and M(NO₂). The barrier heights at the Sulfur atoms reflect the difficulty for electrons to get onto the bridging molecule. From these plots, we might predict that M(H) would have the higher current at a given voltage, followed by M(NO₂), and finally by M(Cl). We will see that calculations of the I-V curves bear this out.

The transmission coefficients for the three molecules are plotted in Fig. 3. The Fermi level has been shifted to zero. An inspection of these plots shows that the HOMO lies close to the Fermi level and at low bias voltage, it will dominate the conduction. Since the addition of NO₂ or Cl shifts the orbitals to lower energy, the HOMO for these molecules is further from the Fermi level than for the parent molecule M(H). Therefore, molecules M(Cl) and M(NO₂) will have lower conduction than M(H) at low voltages. These electron withdrawing groups also shift the LUMO closer to the Fermi level, so that at higher biases the conduction for M(Cl) and M(NO₂) should exceed M(H). The shift to lower energies for molecule M(Cl) is larger

than for molecule $M(\text{NO}_2)$, therefore $M(\text{NO}_2)$ will conduct better than $M(\text{Cl})$ at low voltages, but the larger peaks for the virtual orbitals (1.6-1.7 eV) of $M(\text{Cl})$ suggests that at still higher voltages molecule $M(\text{Cl})$ may have the highest conduction.

Using the transmission coefficients, it is possible to identify conduction channels for the molecules bonded to the metal surfaces. The local density of states (LDOS) gives a spatial profile of these channels. For convenience we refer to the first channels above and below the Fermi level as the HOMO and LUMO channels, respectively. Note however that these channels do not correspond to the HOMO or LUMO orbitals of the parent molecules. The LDOS of the HOMO channel of molecule $M(\text{H})$ is plotted in Fig. 4a. It looks like the HOMO of the free molecule. In Fig. 4b we plot the LDOS for the HOMO channel of all three molecules along the axis of the molecules and where we have integrated over the x and z directions. The $M(\text{H})$ and $M(\text{Cl})$ curves are very similar. The curve for $M(\text{NO}_2)$ shows a larger difference with $M(\text{H})$ than does $M(\text{Cl})$.

In Fig. 5a we plot the LDOS for the LUMO channel of $M(\text{NO}_2)$. As with the LUMO of the free molecule, it is localized mostly on the NO_2 group and the central benzene ring. The integrated local density of states for the LUMO channels of the three molecules are shown in Fig. 5b. As expected, the $M(\text{NO}_2)$ plot is qualitatively different from those for $M(\text{H})$ and $M(\text{Cl})$. It is interesting to note that the local density of states associated with the LUMO channel of $M(\text{H})$ and $M(\text{Cl})$ are more different than are their HOMO channels. This is the reverse of the orbital plots for the free molecules where the LUMOs looked more similar than the HOMOs. Such changes are to be expected since there are significant changes in the molecule associated with bonding to the metal. This is another reminder that while some insight can be obtained from the orbitals of the free molecules, one must show caution and not over interpret the free molecule results. It is more reliable to compute the local density of states.

The computed I-V curves for all three molecules are shown in Fig. 6. Before discussing those computed I-V curves, we note that molecules $M(\text{H})$ and $M(\text{Cl})$ are symmetric, and therefore their I-V curves for positive and negative biases are the same. Molecule $M(\text{NO}_2)$ is asymmetric and therefore its I-V curves for positive and

negative biases are different. Therefore in Fig. 6 we plot the full I-V curve for molecule M(NO₂) with the negative biases plotted as the absolute value of the current to more clearly show the small difference between the positive and negative bias voltages. Free M(NO₂) has a small dipole moment along the backbone (1.11 Debye). While the dipole moment is small, the polarizability along the backbone is very large (922 a₀³), and therefore at relatively low fields (5×10⁻⁴ a.u.), the molecule is stabilized for both a positive and negative field. That is, at low fields the polarizability dominates the dipole moment. Therefore, it is not surprising that there is only a very small difference in the I-V curves at low bias voltage. Yin et al.⁴ also found a small difference between the positive and negative biases for similar molecules. Above 2 V we find a small difference between the positive and negative biases, and rather unexpectedly a crossing of the I-V curves at about 2.7 V. Plots of the transmission coefficients at these biases suggest that at higher voltages (i.e. higher electric fields) the HOMO and LUMO channels are affected differently by the positive and negative fields. If the free molecule is placed in positive and negative electric fields, the valence orbitals mix. For example, the HOMO and HOMO-1 mix and localize one on one side of the molecule and one on the other. The unoccupied orbitals also mix. An inspection of the orbital energies shows that some orbitals are stabilized (or destabilized) by both a positive and negative fields, while some are stabilized by one field and not the other. Given all the changes that occur, it is probably not too surprising that there are some differences in the shape of I-V curves for positive and negative biases. We should also note that in the past we have found²³ bumps in the I-V curves that were related to basis set limitations. It is possible that some of these differences arise from limitations in our ability to describe the distortion induced in the orbitals by the larger fields. However, considering that we are using the valence triple zeta basis set, we suspect that basis set artifacts should be small.

We now focus on comparing the I-V curves for all three molecules. It is fair to say that the computed I-V curves correspond to our expectations based on the zero bias transmission coefficients. Namely, molecule M(H) has the largest current at low bias voltages, but as the bias is increased the values for M(Cl) and M(NO₂) increase, eventually surpassing the values for molecule M(H). We note that our results differ

from previous theoretical results. Taylor et al.³ found essentially no difference in the current for M(H) and M(NO₂). While Yin et al.⁴ did not consider M(NO₂), they considered similar molecules and argued that the conduction was through the LUMO and hence the reduction in the orbital energies by the NO₂ group would increase the current. We are aware of an experimental study by Xiao et al.²² that measured the I-V curves for M(H) and M(NO₂) between 0 and 1.5 V. They found that, in this range of bias values, the current of M(NO₂) was half that of M(H). Our computed results are in good agreement with this. However, we should note that the total current in experiment is about two orders of magnitude smaller than that found in our calculations. This is typical for these types of calculations. In addition, the experimental results of Xiao et al. found NDR at higher voltages for molecule M(NO₂), which we do not see in our calculations.

In Fig. 7 we plot change in charge density at an applied bias of 2 V relative to equilibrium (i.e. no bias). The build up of charge at one end of the molecule is consistent with similar plots for benzene-1,4-dithiol, where only one benzene ring between two Au surface was considered⁸. In that previous work, charge build up near the S atoms resulted in “resistivity dipoles” that impeded current flow. In the molecules we considered, there is, in addition, a significant build up of charge at the C₂ bridging units, showing that they also act as a bottleneck to charge flow. Perhaps these additional C₂ bottlenecks to charge flow help explain why there is a significant difference between the I-V curves for M(H) and M(Cl). In previous work, replacing the H atoms with Cl for a benzene-1,4-dithiol molecule, which has no C₂ bridging units, has only a little affect on the I-V curves.

IV. CONCLUSIONS

We find conduction at low bias values is through the HOMO for the molecules we considered. Therefore the substitution of Cl atoms or an NO₂ group for the hydrogen atoms of molecule M(H) stabilizes the HOMO and reduces the current of the substituted species relative to the parent. This reduction in current for the NO₂ species is consistent with experiment. However, the computed current is about two

orders of magnitude larger than that found in experiment, as is typical for even the highest levels of theory. Analysis of the results shows that both the C₂ bridging units and the thiol anchor groups act as bottlenecks to current flow.

V. ACKNOWLEDGMENTS

C.W.B is a civil servant in the Space Technology Division (Mail Stop 230-3), while J.W.L. is a civil servant in the TI Division (Mail Stop 269-2).

* Electronic address: Charles.W.Bauschlicher@nasa.gov

† Electronic address: John.W.Lawson@nasa.gov

- ¹ J. Chen, M. A. Reed, A. M. Rawlett, and J. M. Tour, *Science* **286**, 1550 (1999).
- ² M.A. Reed, J. Chen, A. M. Rawlett, D.W. Price, and J.M. Tour, *Appl. Phys. Lett.* **78**, 3735 (2001) .
- ³ J. Taylor, M. Brandbyge, and K. Stokbro, *Phys. Rev. B* **68**, 121101(R) (2003).
- ⁴ X. Yin, H. Liu, and J.Zhao, *J. Chem. Phys.* **125**, 094711 (2006).
- ⁵ C. W. Bauschlicher, A. Ricca, Y. Xue, and M. A. Ratner, *Chem. Phys. Lett.* **390**, 246 (2004).
- ⁶ Y. Xue, S. Datta, and M. A. Ratner, *J. Chem. Phys.* **115**, 4292 (2001).
- ⁷ Y. Xue, S. Datta, and M. A. Ratner, *Chem. Phys.* **281**, 151 (2002).
- ⁸ Y. Xue and M. A. Ratner, *Phys. Rev. B* **68**, 115406 (2003).
- ⁹ Y. Xue and M. A. Ratner, *Phys. Rev. B* **68**, 115407 (2003).
- ¹⁰ Y. Xue, Ph.D. thesis, School of Electrical and Computer Engineering, Purdue University (2000).
- ¹¹ D.A. Papaconstantopoulos, *Handbook of the Band Structure of Elemental Solids* (Plenum Press, New York, 1986).
- ¹² A. D. Becke, *Phys Rev A* **38**, 3098 (1988).
- ¹³ J. P. Perdew and Y. Wang, *Phys Rev B* **45**, 13244 (1991).
- ¹⁴ P. J. Hay and W. R. Wadt, *J. Chem. Phys.* **82**, 270 (1985).

- ¹⁵ W. J. Steven, H. Basch, and M. Krauss, *J. Chem. Phys.* **81**, 6026 (1984).
- ¹⁶ M.J. Frisch, J. A. Pople, and J. S. Binkley, *J. Chem. Phys.* **80**, 3265 (1984) and references therein.
- ¹⁷ C. W. Bauschlicher and Y. Xue, *Chem. Phys.* **315**, 293 (2005).
- ¹⁸ C. W. Bauschlicher and J. W. Lawson, *Chem. Phys.* **324**, 647 (2006).
- ¹⁹ A. D. Becke, *J. Chem. Phys.* **98**, 5648 (1993).
- ²⁰ P. J. Stephens, F. J. Devlin, C. F. Chabalowski, and M. J. Frisch, *J. Phys. Chem.* **98**, 11623 (1994).
- ²¹ Gaussian 03, Revision B.05, M. J. Frisch, G. W. Trucks, H. B. Schlegel, G. E. Scuseria, M. A. Robb, J. R. Cheeseman, J. A. Montgomery, Jr., T. Vreven, K. N. Kudin, J. C. Burant, J. M. Millam, S. S. Iyengar, J. Tomasi, V. Barone, B. Mennucci, M. Cossi, G. Scalmani, N. Rega, G. A. Petersson, H. Nakatsuji, M. Hada, M. Ehara, K. Toyota, R. Fukuda, J. Hasegawa, M. Ishida, T. Nakajima, Y. Honda, O. Kitao, H. Nakai, M. Klene, X. Li, J. E. Knox, H. P. Hratchian, J. B. Cross, C. Adamo, J. Jaramillo, R. Gomperts, R. E. Stratmann, O. Yazyev, A. J. Austin, R. Cammi, C. Pomelli, J. W. Ochterski, P. Y. Ayala, K. Morokuma, G. A. Voth, P. Salvador, J. J. Dannenberg, V. G. Zakrzewski, S. Dapprich, A. D. Daniels, M. C. Strain, O. Farkas, D. K. Malick, A. D. Rabuck, K. Raghavachari, J. B. Foresman, J. V. Ortiz, Q. Cui, A. G. Baboul, S. Clifford, J. Cioslowski, B. B. Stefanov, G. Liu, A. Liashenko, P. Piskorz, I. Komaromi, R. L. Martin, D. J. Fox, T. Keith, M. A. Al-Laham, C. Y. Peng, A. Nanayakkara, M. Challacombe, P. M. W. Gill, B. Johnson, W. Chen, M. W. Wong, C. Gonzalez, and J. A. Pople, Gaussian, Inc., Pittsburgh PA, 2003.
- ²² X. Xiao, L. A. Nagahara, A. M. Rawlett, and N. Tao, *J. Am. Chem. Soc.* **127**, 9235 (2005).
- ²³ C. W. Bauschlicher, J. W. Lawson, A. Ricca, Y. Xue, and M. A. Ratner, *Chem. Phys. Lett.* **388**, 427 (2004).

TABLE I: Summary of the electron affinity and orbital energies (in eV) for the three molecules studied in this work, computed at the BPW91 level of theory.

	M(H)	M(NO ₂)	M(Cl)
EA	1.26	1.63	2.13
Orbital Energies			
HOMO-4	-6.487	-6.422	-6.350
HOMO-3	-5.912	-6.177	-6.349
HOMO-2	-5.791	-5.824	-6.231
HOMO-1	-5.791	-5.480	-5.997
HOMO	-5.100	-4.973	-5.533
LUMO	-2.637	-3.324	-3.401
LUMO+1	-1.787	-2.563	-2.470
LUMO+2	-1.186	-1.672	-2.151
LUMO+3	-1.186	-1.265	-2.150
LUMO+4	-1.157	-1.258	-2.090

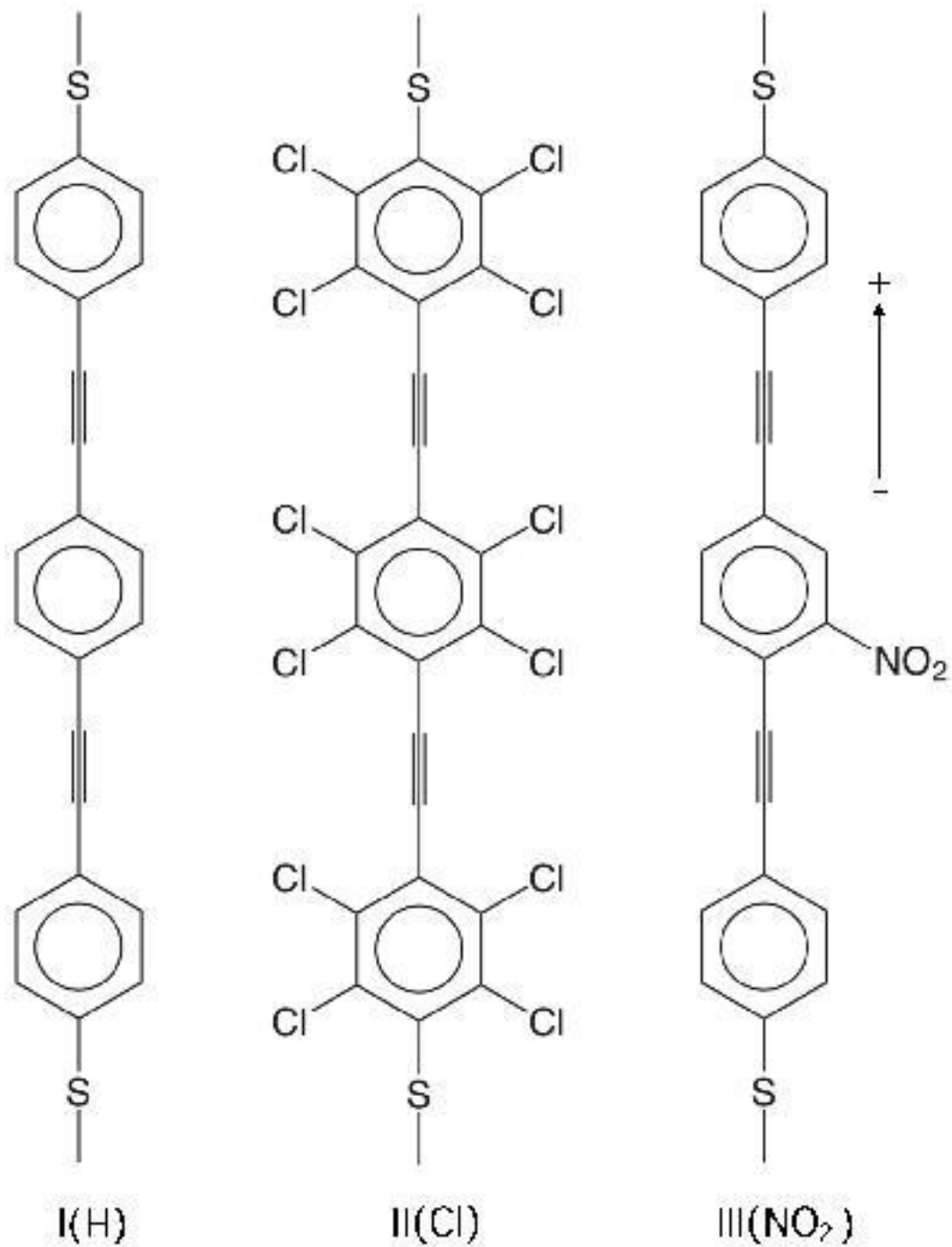


FIG. 1: The three molecules studied in this work. In the free molecule calculations, the ends of the molecule are terminated with H atoms, while in the extended molecule, there are six Au atoms bonded to each of the terminal S atoms. The direction of the dipole moment for molecule NO₂ is shown. A positive bias voltage is defined so that the electric field points in the same direction as the dipole moment.

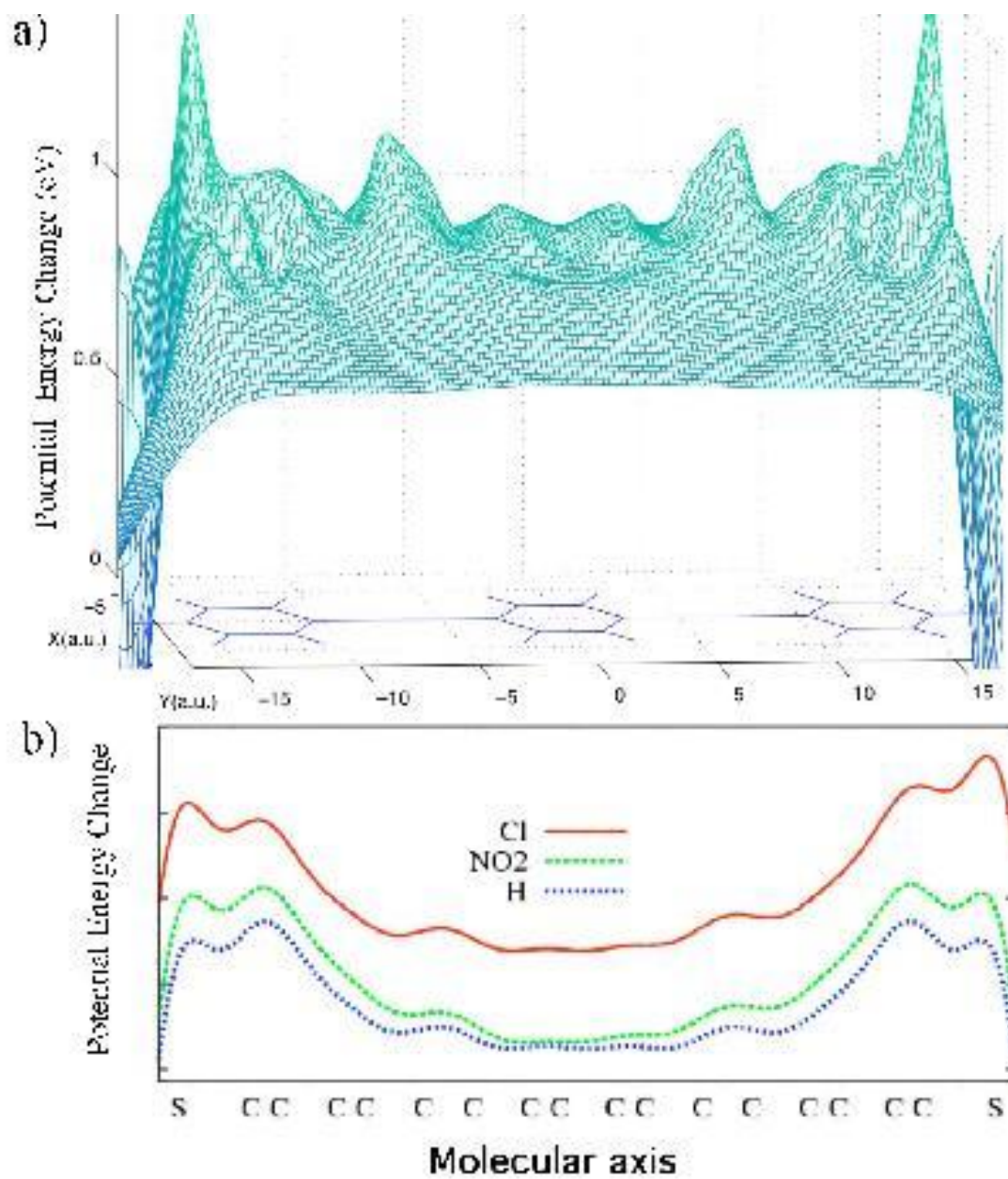


FIG. 2: (Color online) The change in the electrostatic potential energy due to contact formation. a) for molecule I, M(H) and b) a comparison of the 3 species considered in this work.

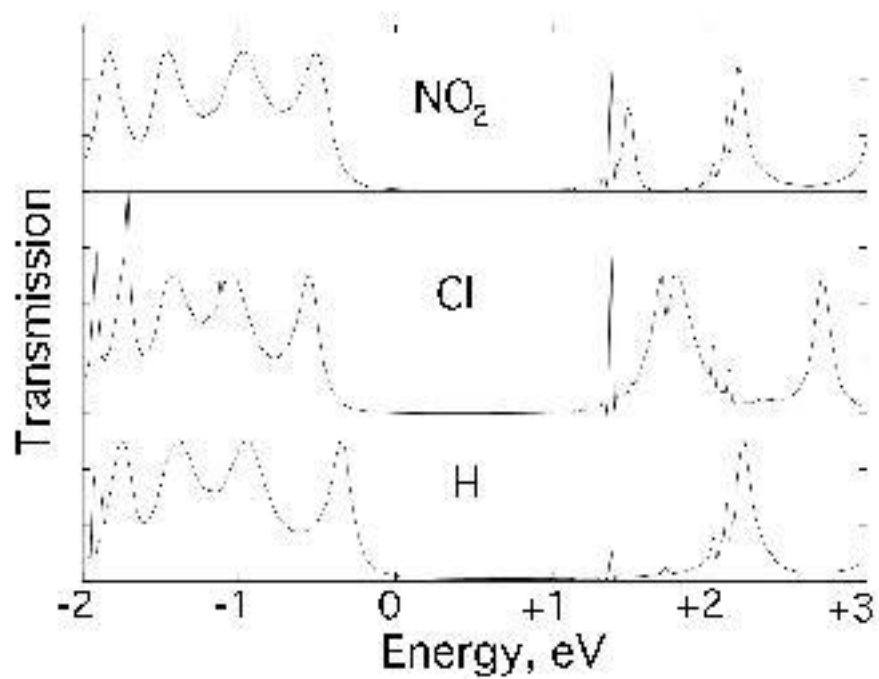


FIG. 3: The transmission coefficient for the three molecules studied in this work. The Fermi level is set to 0.

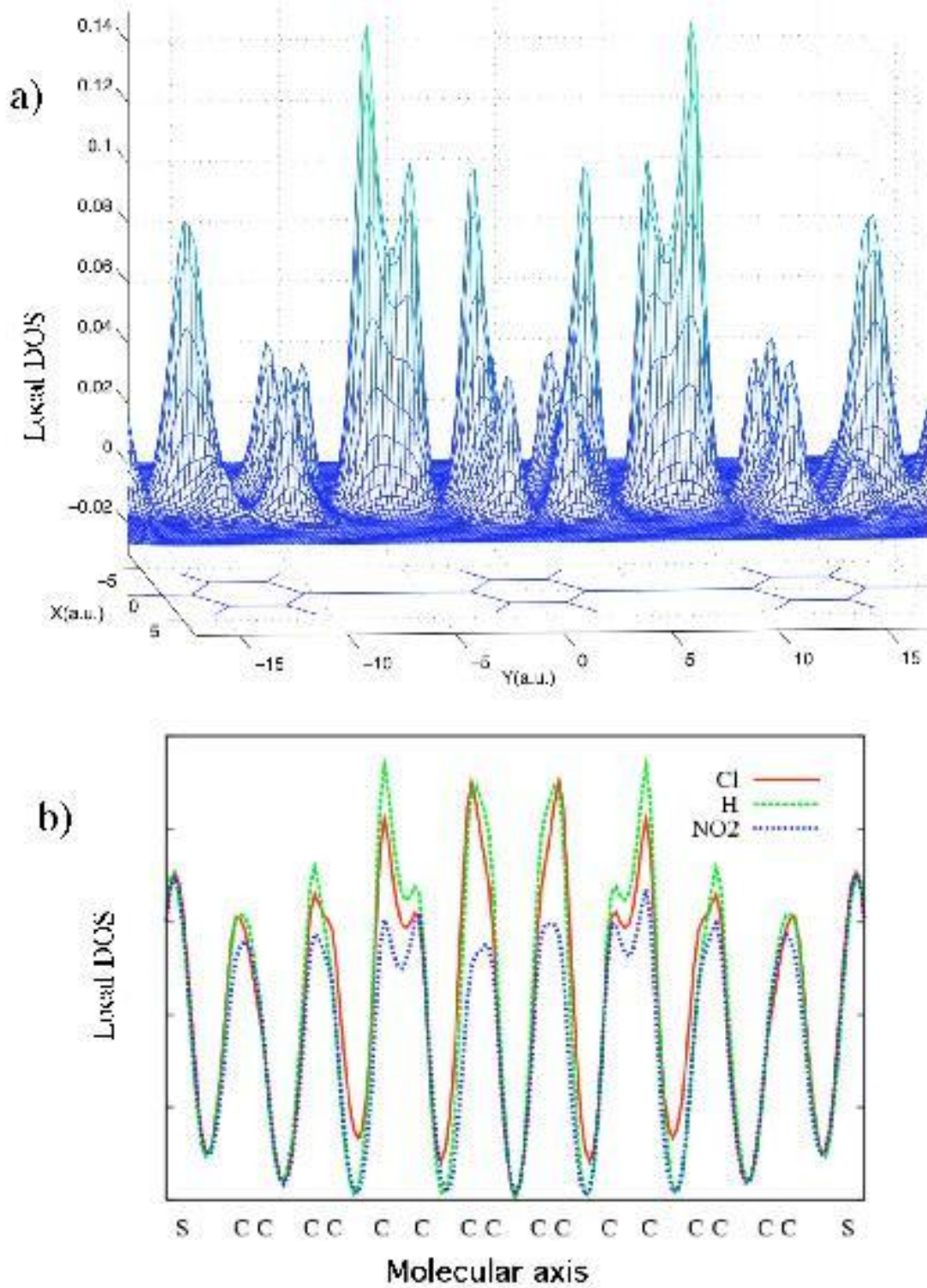


FIG. 4: (Color online) Local density of states for the first channel below the Fermi level. a) for molecule I, M(H) and b) a comparison of the 3 species considered in this work.

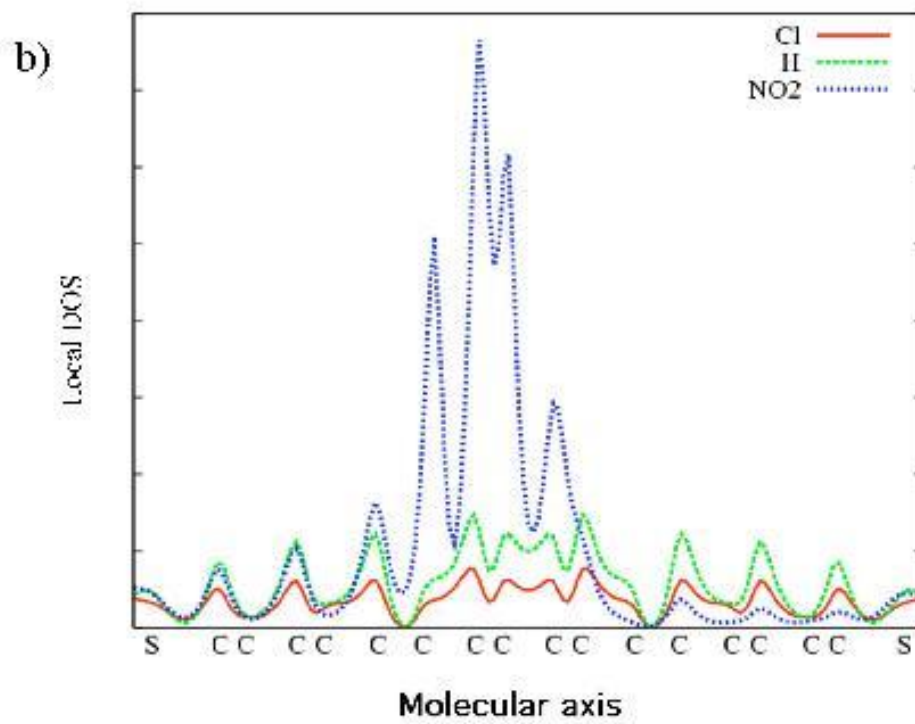
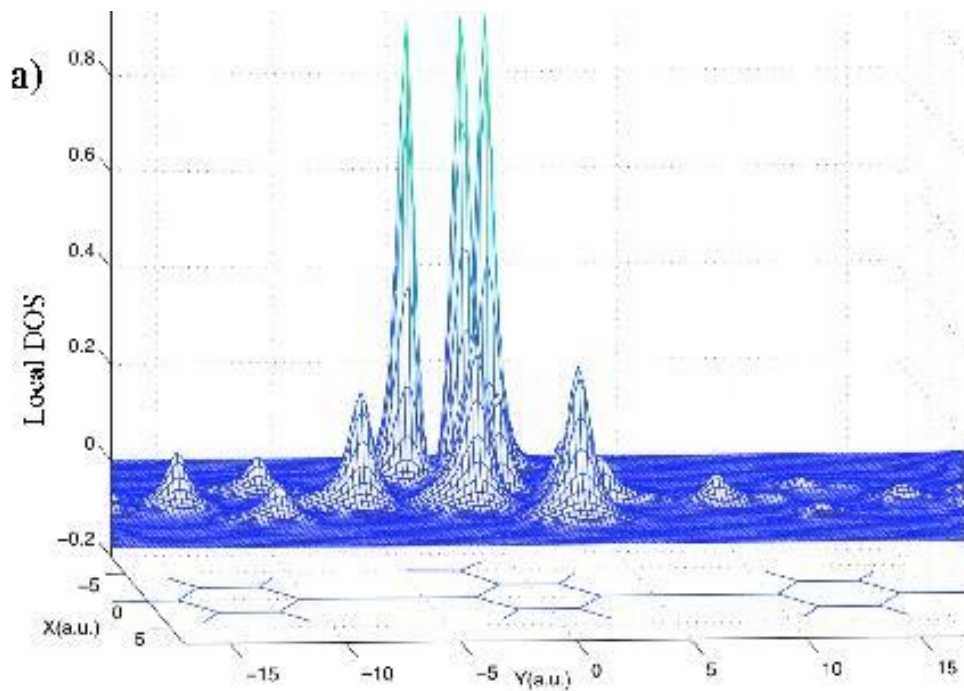


FIG. 5: (Color online) Local density of states for the first channel above the Fermi level. a) for molecule III, $M(\text{NO}_2)$ and b) a comparison of the 3 species considered in this work.

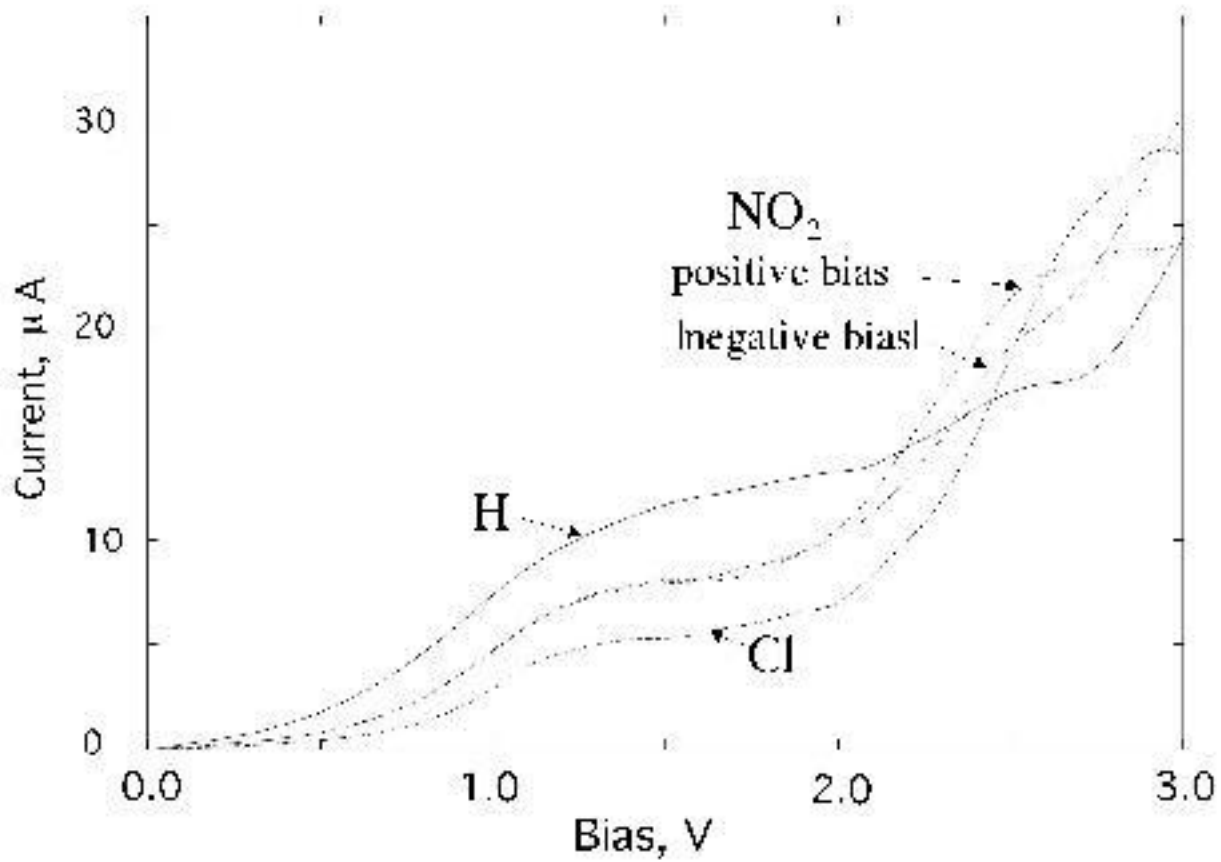


FIG. 6: I-V curves for the three species.

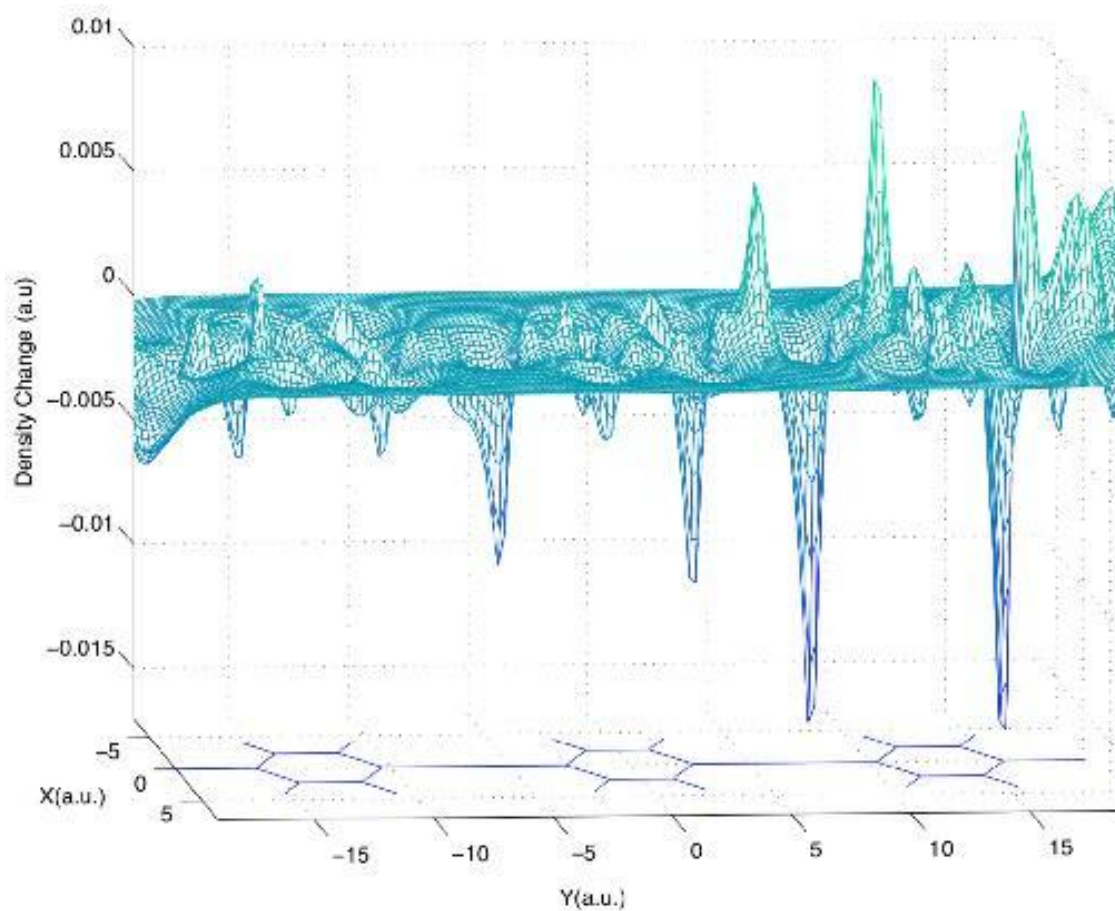


FIG. 7: (Color online) Change in the charge density for molecule I, M(H), for an applied bias of 2.0 V relative to equilibrium.